ELSEVIER

Journal of Chromatography A, 696 (1995) 285–294

JOURNAL OF CHROMATOGRAPHY A

Calculation of the composition of sample zones in capillary zone electrophoresis
II. Simulated electropherograms

J.L. Beckers

Eindhoven University of Technology, Laboratory of Instrumental Analysis, P.O. Box 513, 5600 MB Eindhoven, Netherlands

Received 1 November 1994; accepted 27 December 1994

Abstract

Non-steady-state zone electrophoretic processes can be treated by repeated application of a steady-state mathematical model. Based on this principle, a computer program was set up for the simulation of electropherograms on a temporal basis. Because all parameters of the sample zones can be calculated, all possible detector traces can be simulated. Simulated electropherograms were compared with experimentally determined electropherograms to establish the ability of the mathematical model in qualitative respects. It appears that with this model the fronting and tailing character of sample peaks can be predicted and the reversal of the fronting/tailing character at the point where the mobility of the sample ions equals that of the co-ions. It was remarkable that for strong sample ionic species and applying weak co-ions, the originally tailing character did not change into a fronting character when the mobility of the sample ions exceeded that of the co-ions. Also, the appearance of peaks and dips for the distinguished cases in indirect and direct UV detection can be predicted by the model.

1. Introduction

In Part I [1], a mathematical model was described with which all parameters in sample zones in capillary zone electrophoresis (CZE) can be calculated. The basis of this model is that sample peaks in CZE are divided into small segments with varying sample component concentrations and all parameters of a segment can be calculated from the parameters of the preceding segment with a steady-state model, based on the mass balances of the co- and counter ions, the electroneutrality equation and the modified Ohm's law [2]. In this way, non-steady-state electrophoretic processes can be treated by repeated application of a steady-state model. This model is only usable if electrodispersive effects predominate because other peak-broadening effects, such as diffusion and the influence of the temperature, are neglected. Calculations with this model showed that nearly linear relationships exist between the parameters in the sample peaks, such as the pH, the concentrations of co- and counter ions, the electric field strength and the concentration of the sample component. Although in this model various parameters affecting the electrophoretic separation process are not taken into account, this model gives an insight into the separation process because the changes in all parameters in the sample zones can be calculated.

Electropherograms are generally measured on

0021-9673/95/$09.50
SSDI 0021-9673(94)01297-0

a temporal basis and in order to compare measured and simulated electropherograms, to check the above-mentioned mathematical model, in this work this model was applied for the simulation of electropherograms on a temporal basis. Measured and simulated electropherograms were compared with respect to peak shape, the fronting and tailing character of sample peaks and the question of peaks or dips [3].

2. Theory

Electropherograms are generally measured on a temporal basis, i.e., that at the detector position the trace of a specific parameter is registered. For the simulation of electropherograms this means that it must be calculated how a specific parameter changes in time at the position of the detector. For a UV detector, where the total absorbance of the system is registered, generally concentration profiles of the UV-absorbing components have to be calculated, corrected for differences in molar absorptivities for the different components. For a conductivity detector the trace of the specific conductivity must be calculated.

Calculations with the mathematical model, described in Part I [1], show that different segments of a sample peak, with a different sample component concentration, migrate with different apparent mobilities by the combined effect of differences in the local electric field strength and the effective mobility of the component owing to a change in ionic strength and pH. The apparent velocity of a peak segment i, $v_{\mathrm{app},i}$, is the product of the apparent mobility, $m_{\mathrm{app},i}$, and the electric field strength in the background electrolyte (BGE), E_{BGE}. The apparent mobility is determined by the local effective mobility, $m_{\mathrm{eff},i}$, of the sample component in the peak segment i and the local electric field strength, E_i, and the overall mobility of the electroosmotic flow, m_{EOF}:

$$v_{\mathrm{app},i} = m_{\mathrm{app},i} E_{\mathrm{BGE}} = \left(m_{\mathrm{eff},i} \cdot \frac{E_i}{E_{\mathrm{BGE}}} + m_{\mathrm{EOF}} \right) E_{\mathrm{BGE}} \quad (1)$$

According to this model, the different segments of the sample peak migrate with different velocities and pass the detector at different times, causing the typical triangular sample peaks in CZE. If the mobility of the sample component is higher than that of the co-ions, the velocity of segments with increasing sample component concentrations decrease, through which fronting peaks are obtained. If the mobilities of the sample components are lower than those of the co-ions, tailing peaks are the result. What this means for the development of a sample peak in time and space can be seen in Fig. 1, where the calculated positions of the concentration profiles in the separation capillary are given on a spatial basis for a potassium peak (amount injected $1 \cdot 10^{-11}$ mols) at different times applying a BGE of 0.01 M histidine adjusted to pH 5 by adding acetic acid. The mobilities at infinite dilution and the pK values of all ionic species used in the simulations and experiments are given in Table 1. It can be clearly seen that in course of time (in experiments often after a sample stacking procedure) peaks elute whereby the peaks become broader and the peak heights decrease owing to the electrodispersive character. This means that a sample peak is in dynamic equilibrium. The shape of a sample peak changes in time and a mass transport takes place continuously over all

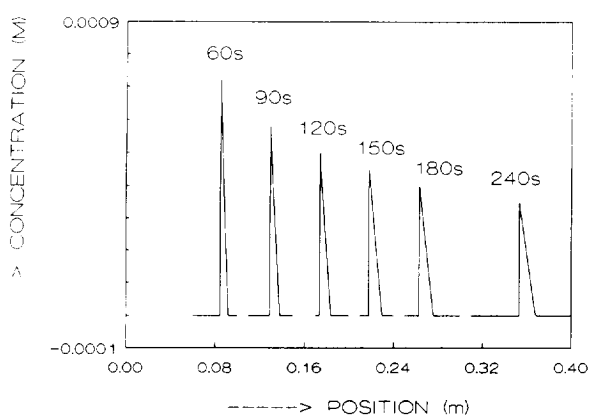

Fig. 1. Development of concentration profiles of a sample peak of potassium (injected amount $1 \cdot 10^{-11}$ mol) in space and time on a spatial basis, applying a BGE of 0.01 M histidine adjusted to pH 5 by adding acetic acid. The numbers refer to the migration times.

Table 1
Ionic mobilities at infinite dilution, m ($m^2/V \cdot s$), and pK values for ionic species used in the simulations and experiments

Ionic species[a]	$m \times 10^9$	pK
Acetic acid	−42.4	4.76
Benzoic acid	−33.6	4.203
Butyric acid	−33.8	4.82
Caproic acid	−30.2	4.857
Formic acid	−56.6	3.75
Histidine	29.7	6.03
Hydrochloric acid	−79.1	−2.0
Imidazole	50.4	6.953
Lithium	40.1	14.0
MES	−28.0	6.095
Sodium	51.9	14.0
Potassium	76.2	14.0
TEA	32.5	>9.0
TMA	43.4	>9.0
Tris	29.5	8.10

[a] MES = 2-(N-Morpholino)ethanesulphonic acid; TEA = tetraethylammonium; TMA = tetramethylammonium; Tris = tris(hydroxymethyl)aminomethane.

peak segments. What this means for the detection of the sample peaks at a specific detector position is illustrated schematically in Fig. 2, where the spatial positions of a peak are shown at times I and II. At time I, the segment with a concentration 1 has reached the detector position. At time II, the segment with a concentration 2 has reached the detector position. During the time interval I–II the shape of the sample peak is changed and in order to know the amount of sample component that has passed the detector at time II, the amount of sample component present in the sample peak beyond the detector position has to be calculated at time II on a spatial basis. The effect of shape deformation is exaggerated in Fig. 2 in order to illustrate this effect.

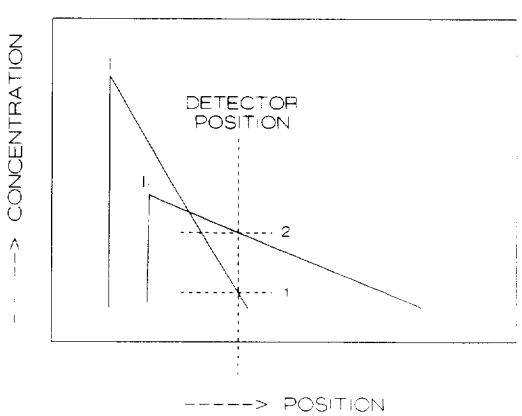

Fig. 2. Concentration profiles of a sample peak at two different times I and II. At time I the peak segment with a concentration 1 is detected whereas at time II the segment with a concentration 2 has reached the detector position. During the time interval I–II the shape of the sample peak changes, i.e., during detection a mass transport takes place continuously over the peak segments.

The calculation of simulated electropherograms on a temporal basis is therefore as follows. First, the relationships between the concentrations of a sample component in a peak segment and various parameters, such as the apparent mobility, concentration of co- and counter ions, electric field strength and specific conductivity, are calculated. In the apparent mobility, deviations in electric field strength are included. Then the velocities of the segments of a sample peak are calculated by applying Eq. 1, starting from the diffuse side of the sample peak. For each time it can be calculated which concentration segment passes the detector position and at that time the amount of sample component Q that already has passed the detector on a spatial basis can be calculated, according to

$$Q = \sum_i A \Delta x_i c_i \qquad (2)$$

with A is the capillary area, Δx_i is the length of the peak segment i and c_i is the concentration of the sample peak in segment i. This procedure is repeated until the sample amount that has passed the detector is equal to the injected amount. The back or front sides of the component peaks are assumed to be sharp. For simulated electropherograms a specific parameter is given in time, dependent on the detector chosen. This procedure can be followed for both fronting and tailing peaks.

3. Experimental

For all CZE experiments a P/ACE System 2000 HPCE apparatus (Beckman, Fullerton,

CA, USA) was used. All experiments were carried out with Beckman eCAP capillary tubing (75 μm I.D.) with a total length of 46.7 cm and a distance between injection and detection of 40.0 cm. The wavelength of the UV detector was set at 214 nm. All experiments were carried out in the cationic mode applying a constant voltage of 10 kV, unless stated otherwise, and the operating temperature was 25°C. Sample introduction was performed by applying pressure injection, where a 1-s pressure injection represents an injected volume of ca. 6 nl and an injected length of 0.136 cm. Data analysis was performed using the laboratory-written data analysis program CAESAR. If experimentally obtained electropherograms are compared with simulated electropherograms, identical values for apparatus parameters are assumed in the simulations. The simulation conditions were as follows: capillary length, 0.467 m; distance between injection and detection, 0.4 m; applied voltage, 10 kV; and capillary diameter, 75 μm.

4. Results and discussion

The mathematical model and the simulation model resting on it must be able to predict both qualitative and quantitative aspects of CZE experiments in order to be useful. The model must be able to predict whether a sample peak will be fronting or tailing, and for weak bases and acids fronting peaks must change into tailing peaks at a specific pH where the effective mobility of the sample ions equals that of the co-ions of the BGE. Sometimes, sample components can be present in electropherograms as a peak or as a dip [3] and the model must be able to predict these effects. Also, quantitative aspects such as the start and end times of the sample peaks, concentrations of the sample component and co- and counter ions, pH, electric field strength and peak area have to be calculated. A problem in the comparison of simulated and calculated values is that calculated values are often based on concentrations, whereas in practice often a UV detector is used, measuring the total UV absorbance of all ionic species. Measured UV absorbances have to be recalculated to concentrations. If only one UV-absorbing component is present, this can easily be done [4]. In the first instance we shall compare calculated and measured electropherograms, focusing on the ability of the model to predict qualitative aspects.

4.1. Peak shape

According to the calculations, the slopes of the concentration profiles of the sample component peaks are independent of, e.g., the concentration of the sample component in the sample solution and sample stacking and/or other concentration procedures. Of course, the maximum concentration in a sample peak cannot exceed the original concentration of the sample component in the sample solution without a sample stacking procedure. To illustrate these effects and to test the model, in Fig. 3 the simulated electropherograms are given for the peaks of the sample components potassium, sodium and lithium applying BGEs consisting of (A) 0.01 *M* histidine and (B) 0.01 *M* imidazole adjusted to pH 5 by adding acetic acid for different injected amounts. Both (1) the concentrations of the co-ions (a measure of the indirect UV signal) and (2) the concentrations of the sample components (a measure of the direct UV signal) are given. Because the mobilities of all sample ions are higher than that of the co-ions histidine, all peaks are fronting and because of the large difference between the mobilities of the sample components and co-ions of the BGE, the effect of electrodispersive effects is great and sample peaks are broad in Fig. 3A. For increasing injected amounts, the diffuse sides of the sample peaks start at the same side. Applying imidazole acetate as the BGE (the mobility of imidazole is just slightly lower than that of sodium), potassium shows a fronting peak and lithium a sharp, tailing peak. For sodium the peak is much steeper and higher, because the electrodispersive character is very small and the diffusion is neglected in the model. Also, the potassium and lithium peaks are narrower and higher than in the case of histidine acetate because the differences between the mobilities of sample ions and

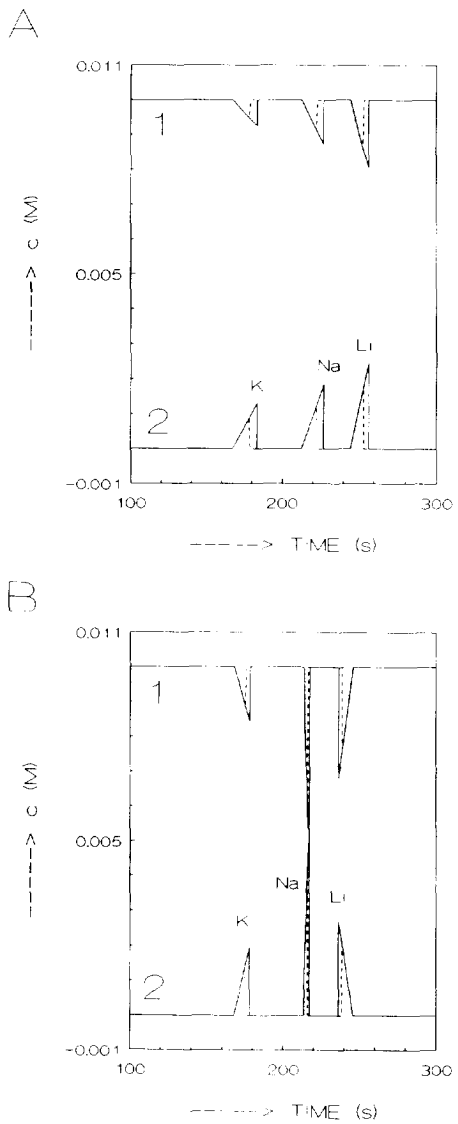

Fig. 3. Simulated electropherograms on a temporal basis for the separation of potassium, sodium and lithium applying BGEs of (A) 0.01 *M* histidine and (B) 0.01 *M* imidazole adjusted to pH 5 by adding acetic acid for injected amounts of (dotted line) $1.1 \cdot 10^{-11}$, (dashed line) $5.5 \cdot 10^{-11}$ and (solid line) $11 \cdot 10^{-11}$ mol. Electropherograms indicated with the number 1 represent the total concentration of the co-ions and gives information about the detector signal applying the indirect UV mode, whereas those indicated with the number 2 represent the total concentrations of the sample components and give an impression of the signal in the direct UV mode. For components with a mobility higher than that of the co-ions fronting peaks are obtained, otherwise tailing peaks. Sample peaks are broader if the mobilities of the components differ much from those of the co-ions.

co-ions are much smaller. In the simulation the m_{EOF} is assumed to be $40 \cdot 10^{-9}$ $m^2/V \cdot s$ arbitrarily and the applied voltage is 10 kV. In the simulations the injected amounts for all components are $1.1 \cdot 10^{-11}$, $5.5 \cdot 10^{-11}$ and $11 \cdot 10^{-11}$ mol, respectively. As can be seen in Fig. 3, the slopes of the sample concentration profiles are always identical for different amounts of sample injected and the diffuse sides start at the same time both for fronting and tailing peaks. To check these aspects experimentally, the potassium peaks were measured carefully, applying a BGE consisting of 0.01 *M* histidine adjusted to pH 5 by adding acetic acid and injecting several different amounts of potassium, dissolved both in water and in BGE. In Fig. 4A the electropherograms are given for (a) the 5-s pressure injection of $1 \cdot 10^{-4}$ *M* and the 10-s pressure injections of (b) $5 \cdot 10^{-4}$ *M* and (c) $1 \cdot 10^{-3}$ *M* solutions of potassium in water. In Fig. 4B the electropherograms are given for 10-s pressure injections of (a) $5 \cdot 10^{-4}$ *M* and (b) $1 \cdot 10^{-3}$ *M* potassium in BGE and 20-s pressure injections of (c) $1 \cdot 10^{-3}$ *M* potassium in BGE and (d) $1 \cdot 10^{-3}$ *M* potassium in water. It can be clearly seen that the slopes of the diffuse sides in all peaks of Fig. 4 are fairly equal. In aqueous solutions the peak height increases, although not linearly, with increasing injected amounts, whereas applying solutions of potassium in BGE a maximum peak height is obtained (Fig. 4B, c) depending on the concentration of potassium in the sample solution. The positions of the diffuse sides can vary owing to a change in mobility of the EOF and a different length of the injection plug.

To check whether the model can predict the change from a fronting peak into a tailing peak, simulations and experiments were carried out for the sample component imidazole in BGEs consisting of 0.01 *M* Tris adjusted to pH 5, 7, 7.5 and 8 by adding acetic acid. In Fig. 5A the measured electropherograms are given for 10-s pressure injections of $5 \cdot 10^{-4}$ *M* imidazole in 10% BGE solution. At a BGE pH of 5 imidazole is fronting whereas the fronting character is changed into a tailing character at pH 7. In Fig. 5B the simulated electropherograms are given for the same cases. For the simulations the m_{EOF}

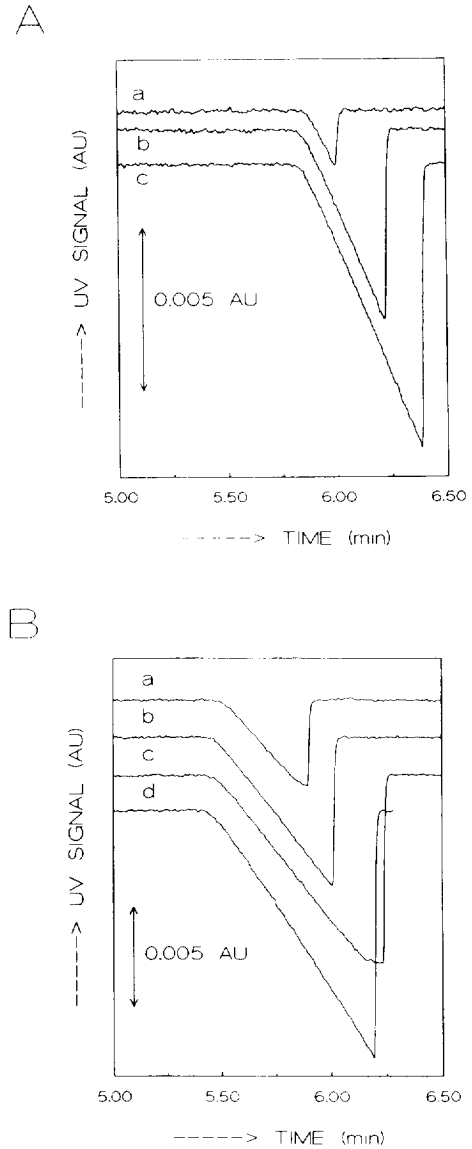

Fig. 4. (A) Electropherograms for (a) 5-s pressure injection of a solution of $1 \cdot 10^{-4}$ *M* potassium ions and 10-s pressure injections of a solution of potassium ions of (b) $5 \cdot 10^{-4}$ and (c) $1 \cdot 10^{-3}$ *M*. The slopes of the concentration profiles of the sample components are equal in all cases. The BGE was 0.01 *M* histidine acetate at pH 5. Applied voltage, 5 kV. (B) Electropherograms for 10-s pressure injections of a solution of potassium ions in BGE for (a) $5 \cdot 10^{-4}$ and (b) $1 \cdot 10^{-3}$ *M* and for 20-s pressure injection of a solution of $1 \cdot 10^{-3}$ *M* potassium ions in (c) BGE and (d) water. The BGE was 0.01 *M* histidine acetate at pH 5. Applied voltage, 5 kV. The slopes of the concentration profiles of the sample component are equal in all cases, for solutions both in water and in BGE.

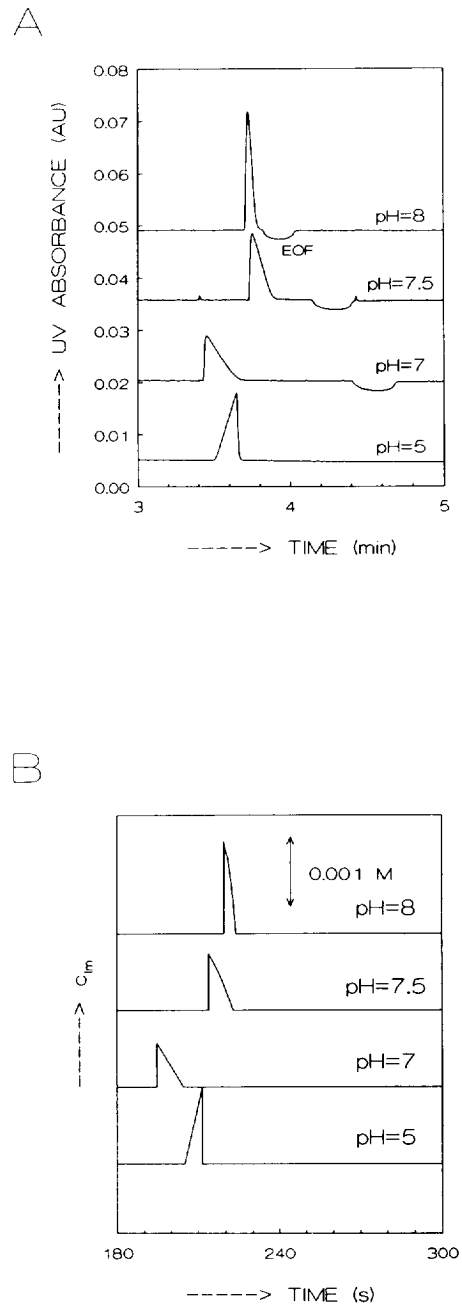

Fig. 5. (A) Measured and (B) simulated electropherograms for 10-s pressure injections of a $5 \cdot 10^{-4}$ *M* solution of imidazole dissolved in 10% BGE solution, applying BGE solution of 0.01 *M* Tris adjusted to different pHs by adding acetic acid. Between pH 5 and 7 the fronting character of the imidazole peaks changes to a tailing character in both the measured and simulated electropherograms. For further information, see text.

values are used as obtained from the experiments. The simulated electropherograms strongly resemble the experimentally obtained electropherograms, although the measured values are based on the direct UV signal whereas in the simulated electropherograms the concentrations of the sample component imidazole are given. The calculated values for the start time of the peaks are generally slightly too small and can be caused because the breakthrough time according to Ref. [5] is not taken into account or from the fact that at $t = 0$ the voltage is not immediately put across the electrodes. This phenomenon is often observed [6].

As a next check on the mathematical model, the sample peak of lithium was calculated applying BGEs consisting of 0.01 *M* imidazole adjusted to different pHs by adding acetic acid. At pH 5, imidazole can be considered as to be fully protonated and its effective mobility will be higher than that of lithium. The lithium peak will be tailing. At pH 7 and higher, the effective mobility of imidazole will decrease and it can be expected that the lithium peak will change into a fronting peak. Surprisingly, in the calculations, the lithium peak maintains a tailing character. The calculated concentration profiles of imidazole (a measure of the UV signal in the indirect UV mode) are given in the simulated electropherograms of Fig. 6A. In the simulations the values of the mobility of the EOF obtained from the measured electropherograms were used. In Fig. 6B the relationships between the calculated apparent mobilities and the pH and the total concentrations of the sample ions in the segments are given for the BGEs 0.01 *M* imidazole acetate at pH 5 and 7. For the BGE of pH 5, the calculated pH (line 4) decreases for an increasing concentration of the sample component and the calculated apparent mobilities (line 2) increase causing tailing sample peaks. For the BGE of pH 7, in first instance the apparent mobilities increased (line 1) with increasing concentration of the sample component, i.e., a peak sharp at the front side and with tailing can be expected, although the effective mobility of the lithium zone is much larger than that of the co-ions in the BGE. At higher concentrations of the sam-

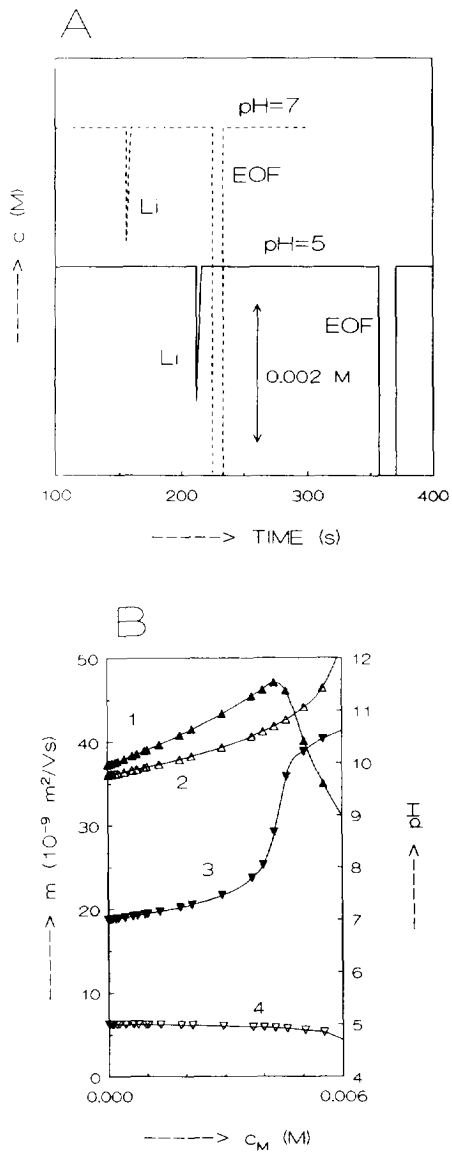

Fig. 6. (A) Simulated electropherograms for lithium applying a BGE of 0.01 *M* imidazole adjusted to pH 5 and 7 by adding acetic acid. Because Li will be measured in the indirect UV mode, the concentration of the co-ions imidazole is given on the electropherograms. In the simulations the Li peaks are tailing in both systems, although the effective mobilities of the co-ions are higher and lower than that of Li at pH 5 and 7, respectively. (B) Calculated relationships between (1, 2) apparent mobilities (left-hand scale) and (3, 4) pH (right-hand scale) of different peak segments in the sample zones and the concentrations of the sample component in the peak segments, for a BGE of imidazole acetate adjusted to (2, 4) pH 5 and (1, 3) pH 7 by adding acetic acid. For further information, see text.

ple component the apparent mobility decreases again, however. For the BGE of pH 7, the pH in the sample zone increase until unrealistic values are reached. What this means in practice is shown in Fig. 7, where the measured electropherograms are given for different injected amounts of lithium applying BGEs consisting of 0.01 *M* imidazole adjusted to a pH of (A) 5 and (B) 7 by adding acetic acid. At both pHs lithium shows a tailing peak. At pH 5 all sample peaks are triangular for different injected amounts of lithium. At pH 7 all peaks are tailing and triangular for not too high injected amounts. On injecting large amounts of sample component, anomalies are obtained. It appears that the sample peak is tailing until a specific concentration is reached, whereas for larger amounts of sample component it migrates as a sharp plug in front of the tailing peak.

4.2. *Peaks or dips?*

Recently, Beckers [3] applied the Kohlrausch regulating function (KRF) and distinguished eight cases in the direct and indirect UV detection modes for fully ionized monovalent ions, assuming identical molar absorptivities for all UV-absorbing ionic species. In several of the cases both UV-transparent and UV-absorbing components could give both peaks and dips, depending on the mobilities of components and co-ions. The mathematical model described must also decisively answer the question of whether peaks or dips can be obtained for all cases, even for weak acids and bases. We therefore simulated and measured electropherograms for some interesting cases. As a first example, the (A) measured and (B) simulated electropherograms are given in Fig. 8 for the separation of a 15-s pressure injection of (1) potassium, (2) sodium, (3) TMA, (4) TEA, (6) caproate, (7) butyrate, (8) acetate and (9) formate ions applying a BGE of 0.01 *M* imidazole adjusted to pH 7 by adding benzoic acid. The concentrations of all sample ions were $2 \cdot 10^{-4}$ *M*, except sodium ($8 \cdot 10^{-4}$ *M*). Because both co- and counter ions are UV absorbing, all sample components are measured in the classical indirect UV mode and therefore the sum of the total concentrations of co- and counter ions is given in the simulated electropherogram. In the measured electropherogram the EOF peak (5) is split and a system peak S is

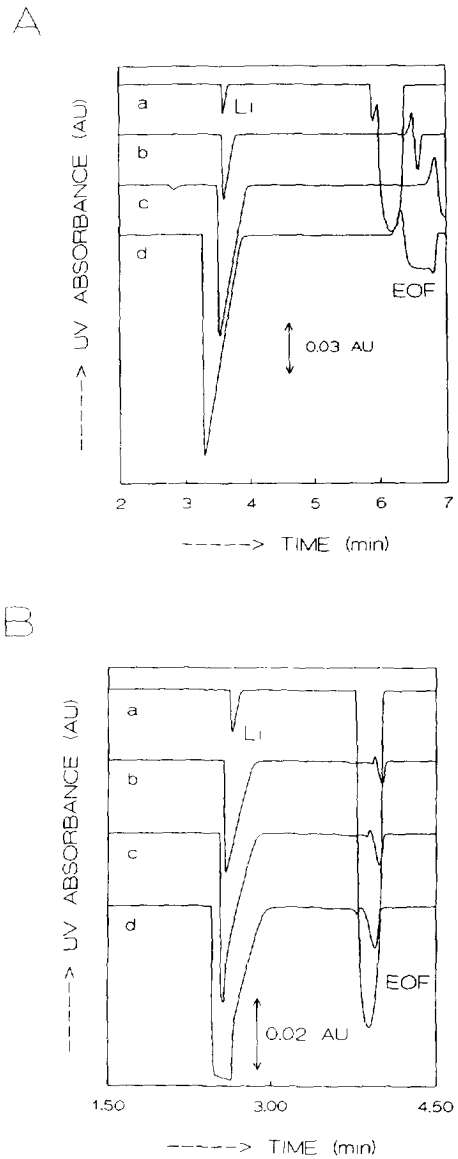

Fig. 7. Measured electropherograms for different amounts of lithium injected applying BGEs of 0.01 *M* imidazole adjusted to pH (A) 5 and (B) 7 by adding acetic acid. The pressure injection times and lithium concentrations were, respectively, (A) (a) 10 s and $5 \cdot 10^{-4}$ *M*, (b) 2 s and $1 \cdot 10^{-2}$ *M*, (c) 10 s and $1 \cdot 10^{-2}$ *M* and (d) 20 s and $1 \cdot 10^{-2}$ *M* and (B) (a) 10 s and $5 \cdot 10^{-4}$ *M*, (b) 3 s and $1 \cdot 10^{-2}$ *M*, (C) 5 s and $1 \cdot 10^{-2}$ *M* and (d) 10 s and $1 \cdot 10^{-2}$ *M*. Applied voltage, 10 kV. For further information, see text.

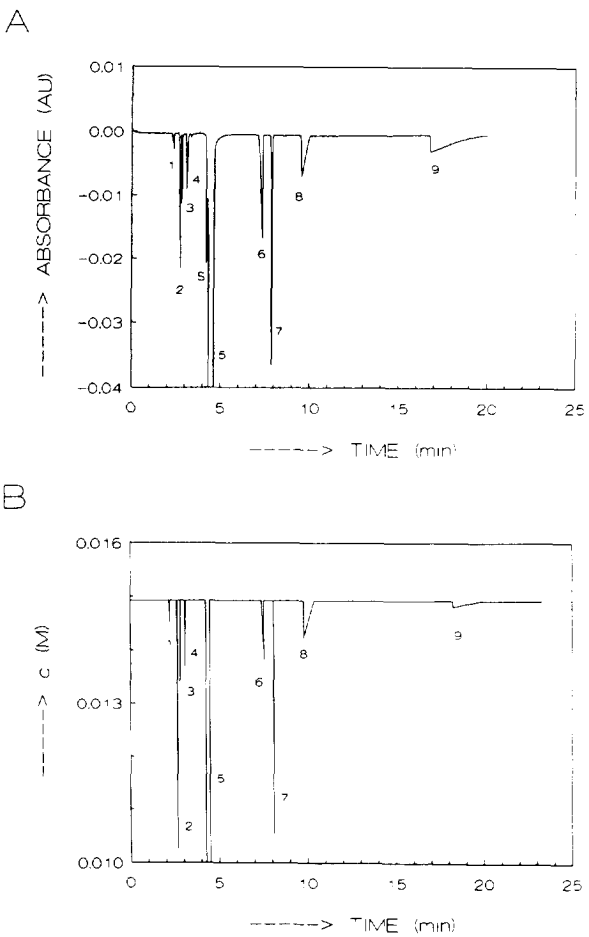

Fig. 8. (A) Measured and (B) simulated electropherograms for the separation of a 15-s pressure injection of (1) potassium, (2) sodium, (3) TMA, (4) TEA, (6) caproate, (7) butyrate, (8) acetate and (9) formate ions applying a BGE of 0.01 *M* imidazole adjusted to pH 7 by adding benzoic acid. The concentrations for all sample ions were $2 \cdot 10^{-4}$ *M*, except for sodium ($8 \cdot 10^{-4}$ *M*). Because both co- and counter ions are UV absorbing, all sample components are measured in the classical indirect UV mode. In the simulated electropherogram the sum of the total concentrations of co- and counter-ions is given. The EOF peak (5) is split and a system peak S is present on the measured electropherogram. For further information, see text.

present [1]. The applied voltage was 10 kV in both the simulated and measured electropherograms. In the simulations the value of the mobility of the EOF obtained from the measured electropherogram was used. In both the measured and simulated electropherograms the sample peaks for the cations and anions with mobilities close to those of the cation (imidazole) and anion (benzoic acid) of the BGE are very sharp and a minimum electrodispersive effect can be observed for these sample components, although this aspect is overestimated in the simulated electropherogram because the diffusion term is neglected in the mathematical model. The very broad peak of formate migrating in the upstream mode, the difference between the mobilities of the sample component and co-ions is large, is remarkable. For all peaks the fronting and tailing character agree in the simulated and measured electropherograms and even the peak shapes and migration times agree well. In Fig. 9 the electropherograms for the separation of the same sample ions are shown, applying a BGE consisting of 0.01 *M* imidazole adjusted to pH 7 by adding acetic acid. In this case the cations are measured in the normal classical indirect UV mode whereby measured peaks resemble the peaks in Fig. 8A. Because the anions of the BGE are UV transparent, in the simulation the concentration of imidazole is given because the UV absorbance will be proportional to this concentration. Again, the EOF peak is split and a system peak S is present in the measured electropherogram. For anions with a mobility higher than that of the co-ions of the BGE, the ionic strength in the sample peak will increase, because the transfer ratio is smaller than one [7], through which also the concentration of imidazole increases, causing an increase in UV absorbance for a UV-transparent component [3]. For this reason, formate is present as a peak in the chromatograms, whereas caproate and butyrate are present as dips. Acetate can not be observed in the electropherogram, because it is present in the BGE.

5. Conclusions

With a simulation model based on a mathematical model described in Part I [1], realistic simulations can be obtained for zone electrophoretic processes whereby the electrodispersive character is the dominant peak-broadening mechanism. All qualitative aspects concerning the peak shape, such as the fronting and tailing

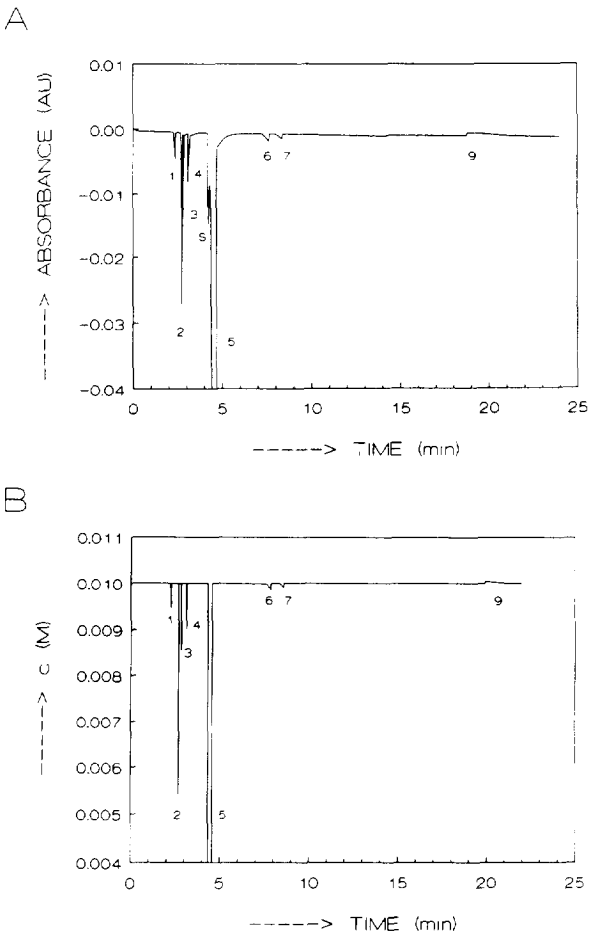

Fig. 9. (A) Measured and (B) simulated electropherograms for the separation of a 15-s pressure injection of (1) potassium, (2) sodium, (3) TMA, (4) TEA, (6) caproate, (7) butyrate, (8) acetate and (9) formate ions applying a BGE of 0.01 *M* imidazole adjusted to pH 7 by adding acetic acid. The concentrations for all sample ions were $2 \cdot 10^{-4}$ *M*, except for sodium ($8 \cdot 10^{-4}$ *M*). Because only the positive ions of the BGE are UV absorbing, all positive ions are measured in the classical indirect UV mode. In the simulated electropherogram the concentration of imidazole is given. In sample peaks of negative ions, with a mobility higher than that of acetate, the ionic strength increases, through which the concentration of imidazole increases, giving an increase in UV absorbance. The EOF peak (5) is split and a system peak S is present on the measured electropherogram. For further information, see text.

character of peaks and the question of peaks and dips, can be predicted. Even anomalies such as the deviating behaviour of lithium in the BGE of imidazole acetate can be seen. Further, all other parameters in the sample peak can be calculated, including concentrations of all constituents, pH and electric field strength. This is in contrast to many other simulation programs or mathematical models. Models based on the KRF [5,8,9] can predict all peak shapes, but generally cannot calculate, e.g., the pH and anomalies in peak shape and baseline disturbances [4]. Also, a recently presented instrument simulator [10,11] for fast graphic illustration of the effect of a large number of variables on the shape of the electropherogram includes many factors but assumes the presence of a BGE, constant in composition, and cannot calculate the various possible UV traces in UV detection.

Quantitative aspects of the mathematical model, such as peak area, peak height and migration times, are currently under investigation.

References

[1] J.L. Beckers, *J. Chromatogr.*, 693 (1995) 347.
[2] J.L. Beckers and F.M. Everaerts, *J. Chromatogr.*, 480 (1989) 69.
[3] J.L. Beckers, *J. Chromatogr. A*, 679 (1994) 153.
[4] J.L. Beckers, *J. Chromatogr. A*, 662 (1994) 153.
[5] F.E.P. Mikkers, *Thesis*, University of Technology, Eindhoven, 1980.
[6] S.V. Ermakov and P.G. Righetti, *J. Chromatogr. A*, 667 (1994) 257.
[7] M.W.F. Nielen, *J. Chromatogr.*, 588 (1991) 321.
[8] E.V. Dose and G.A. Guiochon, *Anal. Chem.*, 63 (1991) 1063.
[9] W. Thormann, *Electrophoresis*, 4 (1983) 383.
[10] J.C. Reijenga and E. Kenddler, *J. Chromatogr. A*, 659 (1994) 403.
[11] J.C. Reijenga and E. Kenddler, *J. Chromatogr. A*, 659 (1994) 417.